HAL
open science

A Fast High Order Arbitrary Lagrangian Eulerian Transformation

Gonçalo Pena, Vincent Chabannes, Christophe Prud'Homme

To cite this version:

Gonçalo Pena, Vincent Chabannes, Christophe Prud'Homme. A Fast High Order Arbitrary Lagrangian Eulerian Transformation. 2011. hal-00657099

HAL Id: hal-00657099

https://hal.science/hal-00657099v1

Preprint submitted on 6 Jan 2012

HAL is a multi-disciplinary open access archive for the deposit and dissemination of scientific research documents, whether they are published or not. The documents may come from teaching and research institutions in France or abroad, or from public or private research centers.

L'archive ouverte pluridisciplinaire **HAL**, est destinée au dépôt et à la diffusion de documents scientifiques de niveau recherche, publiés ou non, émanant des établissements d'enseignement et de recherche français ou étrangers, des laboratoires publics ou privés.

A Fast High Order Arbitrary Lagrangian Eulerian Transformation

Gonçalo Pena[a], Vincent Chabannes[b], Christophe Prud'homme[b]

[a]*CMUC, University of Coimbra, Largo D. Dinis, Apartado 3008, 3001-454 Coimbra, Portugal*
[b]*Laboratoire Jean Kuntzmann, Université Joseph Fourier Grenoble 1, BP 53 38041 Grenoble Cedex 9, France*

Abstract

In this article we propose an arbitrary order Arbitrary Lagrangian Eulerian framework with optimal accuracy and efficiency. The construction is done in two steps, the first one follows the standard construction while the second step builds a high order correction with the solution of a local differential operator, enabling any types of displacements as well as domains shape. Finally we verify on a 3D example that we recover the expected accuracy for first to fourth order geometries.

Keywords: Arbitrary Lagrangian Eulerian, high order methods

1. Introduction

In the context of evolutionary partial differential equations defined in a domain that changes shape over time, the Arbitrary Lagrangian Eulerian (ALE) framework is a well known coordinate system. It allows to keep track of the domain's deformation through a transformation, called the *ALE map*. In this note, we address the construction of such transformation using polynomials of arbitrary degree. In the literature, the reader can find several possible choices to define this transformation in a discrete fashion. Since in most cases we are interested in solving a partial differential equation using a discretization method (finite/spectral element method, for instance), the ALE map that is needed in these calculations is defined in a mesh and is usually a piecewise polynomial belonging to the same approximation space used in the discretization of the PDE. The most common strategy, under the assumption of small displacements, is the use of a harmonic extension operator or a modified version of it, both in the context of piecewise linear finite elements, see Nobile [1], Richter and Wick [2] and Murea and Sy [3], as in their higher order counterpart, see Ho and Rønquist [4]. Another alternative, using arbitrary degree polynomials, suggests the use of a Stokes operator, see Bouffanais [5], to define the so called the *mesh velocity*, and after a time integration procedure, obtain the ALE transformation. This approach has the advantage of defining a divergence free mesh velocity.

Recently, in [6], the authors proposed an arbitrary degree transformation, based on the harmonic extension operator and Gordon-Hall transformations, that has optimal approximation properties with respect to geometry while retaining a low computational cost. However, this methodology is not easily generalized to arbitrary geometrical elements, nor to tridimensional domains.

In the following, we detail the construction of a ALE map, based on the ideas of [6], avoiding the troublesome (implementation-wise) use of Gordon-Hall transformations. The construction of the map is still done in two steps but the second step — formerly the Gordon-Hall transformation — is replaced by a correction built with the solution of a local differential operator, enabling more generality for the type of displacements used, as well as the shape of the handled domains.

2. Notations and preliminaries

Given a elementary simplex domain $K^* \subset \mathbb{R}^d$, $d = 1, 2, 3$, and a positive integer N, let us denote by $\mathbb{P}^N(K^*)$ the space of polynomials of total degree less of equal than N, defined in K^*. We fix a reference element, $\hat{K}$, and consider a transformation $\varphi_{K^*} : \hat{K} \longrightarrow K^*$, called the *geometrical transformation*.

We consider now two domains, Ω^* and $\Omega \subset \mathbb{R}^d$, $d = 1, 2, 3$, which we later refer as the *reference* and the *computational* domains respectively. We further assume that the reference domain has a straight edge/face mesh associated with it, $\mathcal{T}^*$, ie, $\boldsymbol{\varphi}_{K^*} \in \mathbb{P}^1(\hat{K}), \forall K^* \in \mathcal{T}^*$. Furthermore we admit that the mesh $\mathcal{T}^*$ covers exactly the domain Ω^*, *i.e.*, $\Omega^* = \bigcup_{K^* \in \mathcal{T}^*} \overline{K^*}$. We denote $P^N_{c,h}(\Omega^*)$, $\boldsymbol{P}^N_{c,h}(\Omega^*)$ the spaces of piecewise scalar, respectively vectorial, polynomial of total degree N continuous functions in Ω^* and $P^N_{td,h}(\Omega^*)$ the space of piecewise polynomial of total degree N totally discontinuous functions in Ω^*. Let us denote by $\boldsymbol{\eta} : \partial\Omega^* \longrightarrow \partial\Omega$ a displacement function. Through $\boldsymbol{\eta}$, we classify three subsets of the boundary: *(i)* Γ^*_M, the portion of the boundary that moves according to the displacement $\boldsymbol{\eta}$, *(ii)* Γ^*_F, the portion of the boundary that stays fixed (ie, $\boldsymbol{\eta}(\boldsymbol{s}) = \boldsymbol{s}, \forall \boldsymbol{s} \in \Gamma^*_F$) and *(iii)* Γ^*_N, the part of the boundary on which we do not prescribe a displacement, and let the differential operator determine the ALE map freely. The image of each subset, Γ^*_M, Γ^*_F and Γ^*_N by $\boldsymbol{\eta}$ is denoted by Γ_M, Γ_F and Γ_N, respectively. These three sets do not overlap and they verify $\partial\Omega^* = \overline{\Gamma^*_M} \cup \overline{\Gamma^*_F} \cup \overline{\Gamma^*_N}$. To ease the notations, we define $\partial\Omega^*_{\boldsymbol{\eta}} = \Gamma^*_M \cup \Gamma^*_F$ and $\partial\Omega_{\boldsymbol{\eta}} = \boldsymbol{\eta}(\partial\Omega^*_{\boldsymbol{\eta}})$. We introduce now the homeomorphism $\boldsymbol{g} : \partial\Omega^*_{\boldsymbol{\eta}} \mapsto \partial\Omega_{\boldsymbol{\eta}}$ associated to $\boldsymbol{\eta}$ such that

$$\boldsymbol{g}(\boldsymbol{x}^*) = \boldsymbol{x}^* + \boldsymbol{\eta}(\boldsymbol{x}^*), \quad \forall \boldsymbol{x}^* \in \partial\Omega^*_{\boldsymbol{\eta}}. \tag{1}$$

The ALE transformation between the reference and the computational domains is a homeomorphism $\mathcal{A} : \Omega^* \mapsto \Omega$ such that

$$\mathcal{A}_{|_{\partial\Omega^*_{\boldsymbol{\eta}}}} = \mathbf{g}, \quad \mathcal{A}(\Omega^*) = \Omega. \tag{2}$$

3. Construction of the map

We will now assume we are given $\boldsymbol{\eta} \in \boldsymbol{P}^N_{c,h}(\partial\Omega^*_{\boldsymbol{\eta}})$. Our goal in this section is to construct a discrete approximation $\mathcal{A}^N \in \boldsymbol{P}^N_{c,h}(\Omega^*)$ of $\mathcal{A}$ that verifies (2). The construction is in two steps.

The first step is to perform a modified harmonic extension (according to Masud and Kanchi [7]) of the displacement $\boldsymbol{\eta}$ to the interior of Ω^* using piecewise linear polynomial functions. The corresponding ALE transformation, $\mathcal{A}^1$, satisfies

$$\int_{\Omega^*} (1+\tau)\nabla\mathcal{A}^1 : \nabla\mathbf{z}\, dx = 0, \forall \mathbf{z} \in \boldsymbol{P}^1_{c,h}(\Omega^*) \quad \text{and} \quad \mathcal{A}^1 = \boldsymbol{\eta}, \text{ on } \partial\Omega^*_{\boldsymbol{\eta}} \tag{3}$$

where $\tau \in P^0_{td,h}(\Omega^*)$ is defined as follows

$$\tau_{|_{K^*}} = \frac{1 - \frac{V_{\min}}{V_{\max}}}{\frac{V_{K^*}}{V_{\max}}}, \quad \forall K^* \in \mathcal{T}^*.$$

and $V_{\min}$ and $V_{\max}$ are the minimum and maximum volumes of the elements in $\mathcal{T}^*$ and V_{K^*} is the volume of the element K^*. This step is standard in the finite element community regarding the construction of the ALE map.

The second step however is new and is a correction performed in each element K^* whose boundary intersects Γ^*_M in order to build an order N approximation. Denote $\mathcal{T}^{*,b} = \{K^* \in \mathcal{T}^* : \partial K^* \cap \Gamma^*_M \neq \emptyset\}$ the set of elements K^* sharing a face with the boundary of Ω^*, in each element $K^* \in \mathcal{T}^*$ we look for $\mathcal{A}^N_{K^*} \in [\mathbb{P}^N(K^*)]^d$

$$\begin{cases} \displaystyle\int_{K^*} (1+\tau)\nabla\mathcal{A}^N_{K^*} : \nabla\mathbf{z}\, dx = 0, & \forall \mathbf{z} \in [\mathbb{P}^N(K^*)]^d \\ \mathcal{A}^N_{K^*}(\boldsymbol{x}^*) = \boldsymbol{\eta}(\boldsymbol{x}^*) + \boldsymbol{x}^* - \mathcal{A}^1(\boldsymbol{x}^*), & \forall \boldsymbol{x}^* \in \partial K^* \cap \Gamma^*_M \\ \mathcal{A}^N_{K^*} = \mathbf{0}, & \text{elsewhere on } \partial K^*. \end{cases} \tag{4}$$

The final ALE map, $\mathcal{A}^N$ is obtained by adding to $\mathcal{A}^1$ the correction $\mathcal{A}^N_{K^*}$ on each of the elements it concerns

$$\mathcal{A}^N(\mathbf{x}^*) = \mathcal{A}_1(\mathbf{x}^*) + \sum_{K^* \in \mathcal{T}^{*,b}} \mathcal{A}^N_{K^*}(\mathbf{x}^*) + \mathbf{x}^* \tag{5}$$

In order to illustrate the different steps of this construction, we display in Figure 1 the high order mesh construction at each different stages using the following displacement defined at the top and bottom of a rectangular reference domain $\boldsymbol{\eta}^{rect}(\boldsymbol{x}^*) = 0.2\, \exp(\frac{x^*}{5}) \sin\left(\frac{\pi x^*}{2.5}\right) \boldsymbol{n}^*$ where $\boldsymbol{n}^*$ denotes the unit outward normal of the respective reference domains.

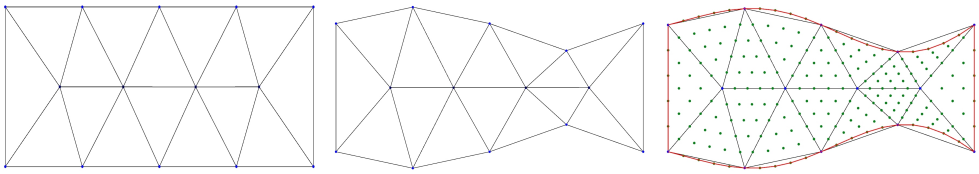

(a) Reference mesh (b) effect of the modified harmonic extension (c) High order correction

Figure 1: Steps to compute the ale map

Proposition 1 (Properties of $\mathcal{A}^N$)**.** *Under the previous assumptions and by construction,* $\mathcal{A}^N \in \boldsymbol{P}^N_{c,h}(\mathcal{T}^{*,b})$ *— enjoys optimal approximation properties* i.e. *the boundary approximation is* $\mathcal{O}\left(h^{N+1}\right)$ *in the* L_2*-norm — and* $\mathcal{A}^N \in \boldsymbol{P}^1_{c,h}(\mathcal{T}^* \backslash \mathcal{T}^{*,b})$.

We discuss now the ALE map construction and proposition 1. First it is clear that the ALE map described previously and the triangulation $\mathcal{T}^*$ induce a triangulation in Ω, $\mathcal{T}$. We highlight also that the construction presented in this paper does not depend on the shape of the elements that the reference triangulation is made of, nor their topological dimension. This has a major impact in the easiness of implementation of this ALE map which can be performed in a wide range of codes.

Another point we would like to stress out is that the operator used to generate the first order ALE map does not have to be the harmonic extension and the whole construction is independent of the choice of the map. In fact, for the overall construction, we are only interested in having a first order ALE map and any other approach can be plugged in. Since in the case of small displacements the modified Laplace equation provides acceptable results, we chose this operator for the presentation in the paper. However, in the more general setting, it fails to provide a usable triangulation $\mathcal{T}$ and other ways of generating the first order ALE map have been considered and used successfully such as the Winslow smoother [8].

Proposition 1 has two important consequences concerning the elements of $\mathcal{T}$: the only elements of $\mathcal{T}$ that have curved edges/faces are located in the boundary of the domain and all the other elements in the triangulation have straight edges/faces. In the framework of Galerkin methods with numerical integration, this feature of the triangulation can provide considerable time savings in the assembly of linear and bilinear forms when compared to a triangulation where all the elements have curved edges/faces. Notice also that the first order ALE map can be computed cheaply and the correction to produce a high order approximation of the domain's boundary is an operation performed elementwise in a small set of elements (compared with the number of elements in $\mathcal{T}$.)

4. Numerical Experiments

We present now some numerical experiments to verify proposition 1. In order to conduct these experiments we use *(i)* Gmsh[9] in order to build the initial high order meshes in 2D and 3D and visualize the meshes computed by our methods and *(ii)* Feel++[10] which provides the framework for arbitrary order Galerkin methods to solve the partial differential equations and handle the computational meshes. Note that the mesh $\mathcal{T}^*$ used to solve equation (3) is built automatically from the initial high order mesh.

As an example of application, we consider the reference domain depicted in figure 2(a) of length 5 and radius 0.5 and the associated displacements at the boundary of each domain $\boldsymbol{\eta}^{cy}(\boldsymbol{x}^*) = 0.2\,\exp(\frac{x^*}{5})\sin\left(\frac{\pi x^*}{2.5}\right)\boldsymbol{n}^*$. Figures 2(b) display the computational domain colored by the corresponding ALE maps.

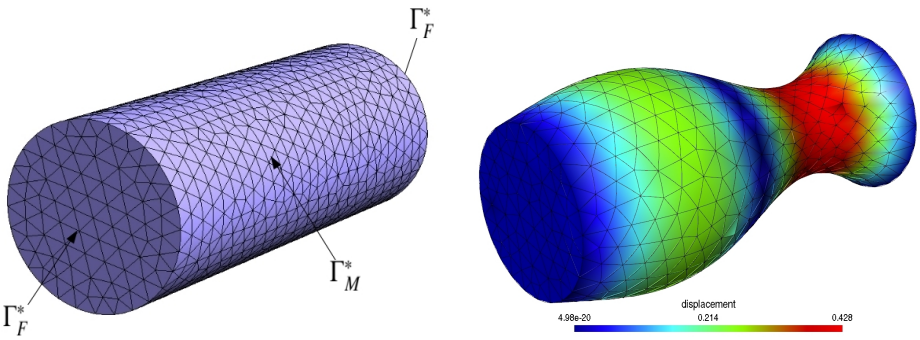

(a) Cylinder, $\Omega^{*,cy}$ (b) Cylinder, $\Omega^{cy} = \mathcal{A}^4(\Omega^{*,cy})$

Figure 2: References meshes (top) and Computational meshes (bottom) of order 4 displayed Gmsh colored by the displacement 2-norm

Finally Figure 3(a) displays the convergence rate of the quantity $\|\mathcal{A}^N(\boldsymbol{x}^*) - (\boldsymbol{x}^* + \boldsymbol{\eta}(\boldsymbol{x}^*))\|_{[L^2(\Gamma_M^*)]^d}$ which confirms the results of Proposition 1. Figure 3(b) represents the convergence rate with respect to geometric order N.

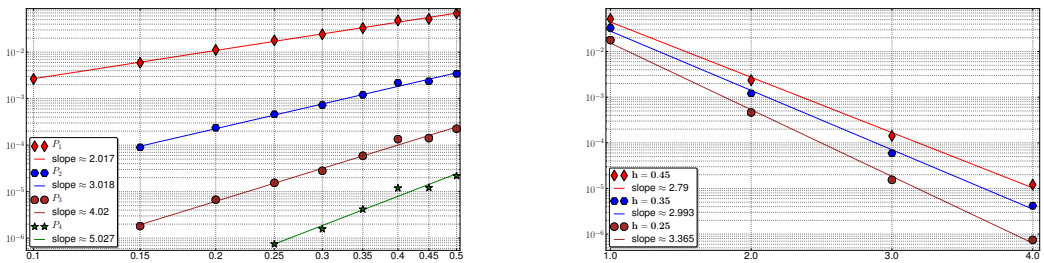

(a) Cylinder (b) Cylinder

Figure 3: Convergence rate plots of $\mathcal{A}^{N,cy}$ (top) and Convergence rate plots of $\mathcal{A}^{N,cy}$ with respect to N (bottom).

Acknowledgements

G. Pena whishes to thank Calouste Gulbenkian Foundation (*Estímulo à Investigação* project). V. Chabannes and C. Prud'homme thank the Region Rhônes Alpes and the projet CHPID for the funding of this work.

References

[1] F. Nobile, Numerical approximation of fluid-structure interaction problems with application to haemodynamics, Ph.D. thesis, EPF Lausanne (2001).

[2] T. Richter, T. Wick, Finite elements for fluid-structure interaction in ALE and fully Eulerian coordinates, Computer Methods in Applied Mechanics and Engineering 199 (41-44) (2010) 2633–2642.

[3] C. M. Murea, S. Sy, A fast method for solving fluid-structure interaction problems numerically, Int. J. Numer. Meth. Fluids 60 (2009) 1149–1172.

[4] L. W. Ho, E. M. Rønquist, Spectral element solution of steady incompressible viscous free-surface flows, Finite Elem. Anal. Des. 16 (3-4) (1994) 207–227.

[5] R. Bouffanais, Simulation of shear-driven flows: transition with a free surface and confined turbulence, Ph.D. thesis, EPF Lausanne (2007).

[6] C. Prud'homme, G. Pena, A. Quarteroni, High order methods for the approximation of the incompressible Navier-Stokes equations in a moving domain, Comput. Meth. Appl. Mech. Eng.To appear.

[7] H. Kanchi, A. Masud, A 3D adaptive mesh moving scheme, International Journal for Numerical Methods in Fluids 54 (6-8) (2007) 923–944.

[8] A. Winslow, Numerical solution of the quasilinear poisson equations in a nonuniform triangle mesh, J. Comp. Phys. 2 (1967) 149–172.

[9] C. Geuzaine, J.-F. Remacle, Gmsh: a three-dimensional finite element mesh generator with built-in pre-and post-processing facilities, International Journal for Numerical Methods in Engineering 79 (11).

[10] C. Prud'homme, V. Chabannes, G. Pena, Feel++: Finite Element Embedded Language in C++, Free Software available at http://www.feelpp.org, contributions from A. Samake, V. Doyeux, M. Ismail and S. Veys.